U.S. DEPARTMENT OF COMMERCE
NATIONAL OCEANIC AND ATMOSPHERIC ADMINISTRATION
NATIONAL WEATHER SERVICE
NATIONAL METEOROLOGICAL CENTER

OFFICE NOTE 317

A COMPARISON OF FORECAST GUIDANCE DERIVED FROM ISENTROPIC AND SIGMA COORDINATE REGIONAL MODELS

THOMAS BLACK
VISITING SCIENTIST, DEVELOPMENT DIVISION

FEBRUARY 1986

A Comparison of Forecast Guidance Derived from Isentropic and Sigma Coordinate Regional Models

Abstract

Forecasts from an isentropic coordinate model employing a sigma coordinate subdomain are compared with those from two of the National Weather Service's operational models, the LFM II and the NGM. Five significant weather events are considered with attention given to those predicted quantities most important to each case. While the isentropic model forecasts displayed various strengths, the most notable was the superior description of water vapor transport in the vicinity of frontal convection, a characteristic suggesting potential applications toward improved severe weather and precipitation prediction.

1. Introduction

Throughout the history of numerical weather prediction, pressure or pressure-related quantities have been favored as the vertical coordinate in model atmospheres. Charney, et al. (1950) produced the first successful dynamical-numerical prediction using an equivalent barotropic model, essentially describing conditions at the 500 mb level. Phillips (1957) realized the advantage of normalizing the pressure coordinate and his proposed sigma system has achieved widespread use. The linearity of both the pressure gradient force and the continuity equation provide the mathematical advantage of isobaric coordinates while the terrain-following nature of sigma coordinates removes major problems associated with lower boundary conditions.

Although potential temperature (θ) as the vertical coordinate enjoys less popularity than the pressure-based systems, isentropic coordinates continue to attract attention due to their physically useful dscription of

motion and stability. Above the lower boundary a sigma surface reflects nothing of the physical nature of atmospheric motion. In contrast an isentropic surface describes the locus of trajectories of all parcels which initially possess a given potential temperature and which move under adiabatic, frictionless conditions. On the synoptic scale this renders motion virtually two-dimensional thereby reducing truncation errors and isolating the generally small diabatic and frictional effects. In addition, enhanced vertical resolution in θ-space exists in regions of large static stability through Poisson's relation. While the utility of θ-coordinates in objective analysis has been realized for decades (Rossby, et al., 1937; Danielsen, 1959; Shapiro and Hastings, 1973; Petersen, 1979), their introduction to prediction models has been more recent. Since the first successful integration of the primitive equations in isentropic coordinates by Eliassen and Raustein (1968), such prediction models have been used in frontogenesis studies (e.g. Shapiro, 1975; Macpherson, et al., 1980; Buzzi, et al., 1981) and in the related area of numerical simulation of jet streak circulations (Gall and Johnson, 1977; Uccellini and Johnson, 1979; Black, 1984). Subsequent to the work of Eliassen and Raustein, additional but limited development of more general isentropic coordinate forecast models has taken place (Bleck, 1974, 1977; Deaven, 1976).

This paper will summarize results from an experimental primitive equation model constructed as an isentropic coordinate analog to the National Weather Service's sigma coordinate Limited Area Fine Mesh Model (LFM II). In order to determine if the theoretical advantages of θ-coordinates might manifest themselves as significant improvements in forecast fields, five test runs from the isentropic model will be compared with identical runs from the LFM, and in four of the cases, from the sigma coordinate Nested Grid Model (NGM), the prediction component of the National Weather Service's Regional Analysis

and Forecast System. After a brief description of the isentropic model, results from the series of forecasts generated by the models will be compared. A variety of significant weather events was selected which include: Two springtime severe weather outbreaks (Cases 1 and 2); a late summer isolated convective cluster (Case 3); an early winter arctic cold surge (Case 4); explosive late winter East Coast cyclogenesis in the President's Day storm (Case 5). NGM forecasts were available in Cases 2 through 5. The intention of the following discussions is not to present formal case studies but to assess the quality of the guidance offered by the prediction models through the forecast fields most important to the particular event being considered.

2. Characteristics of the Isentropic Model

Two major problems associated with isentropic coordinates concern conditions near or at the lower boundary. Isentropic surfaces tend to intersect the ground even more steeply than isobaric surfaces and in regions of strong surface heating isentropes often fold thereby destroying vertical monotonicity. One method of ameliorating these difficulties is use of a hybrid approach (Deaven, 1976; Gall and Johnson, 1977) and involves insertion of a sigma coordinate subdomain beneath the isentropic coordinate domain so as to preclude intersection of coordinate surfaces with the ground, allow for easier handling of complex terrain, and locate low level superadiabatic regions within a coordinate domain where such conditions can be described. In the model, sigma is defined as

$$\sigma = \frac{p - p_1}{p^*}$$

where p_1 represents the pressure on the uppermost sigma surface and p^* is the constant difference between surface pressure and that on the uppermost sigma surface.

A vertical cross section of the domain is seen in Fig. 1. The sigma coordinate subdomain consists of two predictive surfaces located 50 mb and 100 mb above the ground. The remainder of the domain is described by ten isentropic coordinate surfaces reaching from the uppermost sigma surface to 420K. Above this level is an assumed barotropic region with no vertical windshear. The initial conditions determine the vertical resolution in the troposphere ($\Delta\theta_{TR}$) through an equal division of the difference between 345K and the mean potential temperature on the uppermost sigma surface along an east-west row in the middle of the domain. Typically $\Delta\theta_{TR}$ is about 10K. In the stratosphere where the static stability is greater, the vertical resolution $\Delta\theta_{ST}$ equals 25K for all cases. The horizontal domain is a polar stereographic projection covering North America and adjacent waters and is identical to that of the LFM. There are 45 by 53 grid points at a 190.5 km resolution. Spatial derivatives are approximated using the semi-momentum method of Shuman (1962), a modified central difference technique which conserves momentum and suppresses nonlinear instability. An explicit diffusion term of the form $K\nabla^2\eta$ is included in the prediction of primary quantities. Horizontal boundary conditions at time t are determined precisely as in the LFM, that is, from the predicted tendencies in the hemispheric spectral model for time t-12 hours. Integration is centered in time with Δt=300s. The initial conditions are derived from the LFM analysis by interpolation from the mandatory pressure levels onto σ and θ-coordinate surfaces. A direct isentropic analysis has also been tried but the forecasts appear relatively insensitive to the type of analysis used.

Precipitation calculations include both large scale and subgrid algorithms. The subgrid scheme produces rainfall if there is moisture convergence, if the relative humidity exceeds 75%, and if the environment is sufficiently unstable.

The resultant latent heat is released in the layer above although there is no exchange of water vapor between layers in this routine. Bulk evaporation of falling rain is permitted on large scale precipitation only. Vertical transport of sensible heat and moisture is described over the ocean's surface but ignored over land.

3. Test Forecasts

The date and hour heading on each of the following cases refers to the initial time of the model forecasts. Because of the frequency and impact of intense frontal-related convection, both Cases 1 and 2 will involve this type of activity. In such an event moisture is a key variable to both the researcher due to dynamic and thermodynamic implications and to the public through precipitation forecasts. While only the moisture forecasts from the 36-hour forecasts (coinciding with the period of peak activity) will be displayed in these two cases, other significant differences between the models which may have occurred will also be pointed out.

a. Case 1: 12Z May 10, 1985

At the beginning of the forecast period a cold front reached southwestward from a 992 mb low in Labrador becoming stationary over Upper Michigan and extending through two weak low pressure centers in South Dakota and southern Utah. After 24 hours the surface low in South Dakota had become dominant and moved slowly into the eastern part of the state trailing a cold front through eastern Nebraska and down through the Texas panhandle. A 500 mb trough had moved rapidly eastward and now possessed a voriticy maximum of 18×10^{-5} s^{-1} over northeast Colorado.

By 00Z May 12, the 500 mb trough had lifted to the northeast and its associated vorticity maximum of 18×10^{-5} s^{-1} was located over northeast Nebraska. The surface low in South Dakota had moved only slightly to the east

and the trailing cold front was now pushing into western Iowa. Several hours earlier at approximately 20Z a squall line formed east of the front along the strong moisture gradient in central Iowa and moved eastward producing severe thunderstorms with damaging winds and several tornadoes. While surface pressure and thickness fields were relatively well forecast by both models, the LFM predicted a broader, less intense vorticity maximum in North Dakota much further north than analyzed while the isentropic model accurately forecast a vorticity maximum of 18×10^{-5} in eastern Nebraska.

Vertical velocity is quantified in the isentropic model only in terms of K s^{-1} and not mb s^{-1} thus an indirect approach was used to judge vertical motion forecasts. Since from a quasi-geostrophic viewpoint upward motion resulting from positive differential vorticity advection could have played a role in producing an environment conducive to the formation and maintenance of the intense convection, the vorticity advections derived from the 500 mb and 300 mb analyzed and forecast wind fields at 00Z May 12 were inspected. The results indicate a PVA maximum at 500 mb of roughly 2.5×10^{-9} s^{-2} over south central Iowa as determined from the analyzed winds. The LFM accurately produced much weaker PVA over Iowa with a maximum of only 0.5×10^{-9} s^{-2} located over central Wisconsin. Winds forecast by the isentropic model yielded PVA over all of Iowa with a 2.0×10^{-9} s^{-2} maximum over the central part of the state. At 300 mb the centers of vorticity advection were over nearly the same locations with values of 4.0×10^{-9}, -2.0×10^{-9}, and 2.5×10^{-9} for the analyzed, LFM, and isentropic model winds, respectively. Such diagnostic suggest that the isentropic model may have more accurately described synoptic scale upward motion in the region of activity ahead of the advancing cold front.

Moisture forecasts at the 36-hour time period indicated that same contrasts between the models that had occurred at 24 hours. The mean relative humidities depicted in Fig. 2 show a remarkable similarity between the analyzed and isentropic model fields, best exemplified perhaps by the location of the 50% and 70% isopleths. Note the southward extension of 50% RH into eastern Texas and of 70% RH into Illinois and Indiana. In contrast the LFM predicted anomalously dry air over the Ohio Valley and into the upper midatlantic states. The analyzed specific humidity at 850 mb (Fig. 3a) again reveals the moisture tongue ahead of the cold front and shows a broadening to the east. The LFM (Fig. 3b) still failed to describe the strong frontal gradient and produced values too dry over most of the eastern U.S. The isentropic model (Fig. 3c) did show the frontal gradient and except for an incorrect maximum of 12g kg^{-1} in northwest Wisconsin, produced a relatively accurate description of water vapor east of the front.

Fig. 4 shows the observed and forecast precipitation fields for 24 hours ending 00Z May 12. Observations clearly show the heavier amounts in southeast Iowa associated with the squall line and the broad area of rainfall in North Dakota and Minnesota associated with the low pressure center. The LFM succeeded in describing much of the large scale precipitation to the north and even predicted a small local maximum over southern Iowa (not seen in Fig. 4 due to the contour interval). Rainfall around the low was also predicted by the isentropic model but it occurred too far north and east in southern Manitoba and Ontario. No maximum associated with the convection in Iowa was indicated.

b. Case 2: 12Z May 30, 1985

In this second test involving intense convection all forecast fields were also available from the NGM. At the initial time of the model forecasts

two low pressure centers separated by a stationary front were located in upper Michigan and western South Dakota, the former with a leading warm front across eastern Michigan into Ohio and the latter with a trailing cold front across western Nebraska, Colorado, and Utah. After 24 hours the Michigan low had moved into southern Quebec and weakened while the other center had intensified and moved into northern Wisconsin with an associated cold front stretching into Indiana and southern Illinois then southwest into the Texas panhandle.

By 36 hours the primary low had moved into eastern Ontario and the cold front had reached northwest Pennsylvania. At approximately this time severe thunderstorms were occurring across western Pennsylvania accompanied by numerous tornadoes. The mean relative humidities in Fig. 5 depict the same relationships between analysis and forecasts as at 24 hours. Whereas the isentropic model forecast captures a region of RH>70% along the East Coast reasonably similar to that analyzed although again extending it too far south, the only indication of such as area in the LFM forecast is a slight dip in the 70% line into Massachusetts and the 50% line into Tennessee. The NGM did somewhat better than the LFM in that the 50% RH isopleth extended as far south as the Florida panhandle although the 70% line barely reached into Connecticut. The 850 mb specific humidity fields at 36 hours are shown in Fig. 6. A broad area of 12g kg^{-1} stretches from Arkansas northeastward to New York with a 14g kg^{-1} region lying between central Tennessee and Maryland. The LFM predicted a field oriented more meridionally ahead of the front and the specific humidity values in the key area of activity in Pennsylvania were about 10g kg^{-1} or roughly 3g kg^{-1} less than in the analysis. The NGM showed a very similar region of magnitudes greater than 10g kg^{-1}. The isentropic model predicted values >12g kg^{-1} over an extensive region in advance of the cold front similar to that analyzed with almost identical values in Pennsylvania.

Observed and forecast 24-hour rainfall ending 00Z June 1 are shown in Fig. 7. The actual precipitation associated with the severe weather is seen in northeast West Virginia and extending across western Pennsylvania. While the LFM did not clearly indicate the relatively localized areas of heavy rainfall, small local maxima not see in Fig. 7b were predicted over southern Ohio and western Pennsylvania. The NGM missed the severe convection but did accurately place maxima in eastern North Dakota and eastern Michigan. Although the isentropic model was the only one to predict amounts exceeding one inch, the region over the Great Lakes in which it did so included none of the locations where such amounts were observed.

c. Case 3: 12Z September 28, 1983

At the time of initialization of the forecast models, a cold front associated with low pressure centers in central and northern Canada was moving across the Great Plains while a secondary low was forming in Colorado. Although advancing rapidly eastward in Canada, the front proceeded slowly across Nebraska reaching the vicinity of Omaha 24 hours after the initial time. This case is somewhat unique in that the synoptic scale features were predicted quite accurately by all three models. The primary challenge in this forecast was providing guidance for a major precipitation event in south central Nebraska the magnitude of which can be seen in the 24-hour observed rainfall amounts ending 12Z September 28 shown in Fig. 8a. The national radar summary indicating conditions near the end of the 24-hour forecast period is presented in Fig. 8b. A nearly stationary cluster of heavy thunderstorms forming early in the period was responsible for the heavy precipitation.

Figs. 9 and 10 show the two consecutive 12-hour rainfall forecasts. The LFM indicated no precipitation whatsoever in Nebraska or Kansas during the first period. In fact that model's predicted mean RH field had a minimum

of <50% in southwest Nebraska. In contrast the NGM did predict an area of light precipitation with a very small local maximum of 0.05 inches at precisely the correct location (not seen in Fig. 9b). An extensive area of light precipitation along the entire length of the cold front was predicted by the isentriopic model although a maximum of 0.15 inches was indicated in east central Nebraska. Fig. 8b shows that at the end of the second 12-hour period the primary activity was still located near the Nebraska-Kansas border with weaker cells along the front in northwest Iowa and south central Minnesota. The forecasts for this period (Fig. 10) show that the only maximum near the front in the LFM was found in northwest Wisconsin. The NGM had only very light rain in southern Nebraska and had moved its heaviest precipitation into southwest Minnesota. As in the LFM, the isentropic model produced light rain all along the front but still maintained a maximum in central Nebraska, relatively close to the actual convection.

As stated previously the synoptic scale pressure, wind, and moisture fields were with few exceptions very similar in all three model forecasts implying that differences between the precipitation routines and subgrid scale parameterizations were likely important for the variations in the predictions. However, a difference that occurred in the upper level divergence fields may partly explain the isentropic model's maintaining a larger rainfall maximum in Nebraska. Fig. 11 shows the velocity divergence at 300 mb for the analyzed and forecast winds. The analysis shows a maximum divergence of over 2.0×10^{-5} s^{-1} over northern Nebraska. The LFM produced a maximum of $\sim 1.5 \times 10^{-5}$ s^{-1} over North Dakota while the NGM indicated a region with values $>0.5 \times 10^{-5}$ s^{-1} coinciding fairly closely with the position of the front. The isentropic model though produced a divergence maximum of $\sim 1.8 \times 10^{-5}$ s^{-1} at nearly the same location as in the analysis. Through continuity the stronger velocity

divergence aloft could enhance or sustain the upward motion occurring below and thus augment precipitation formation.

d. Case 4: 12Z December 22, 1983

While previous cases have focused on moisture and precipitation, the primary forecast problem in this case is that of properly predicting the surface pressure pattern associated with a major outbreak of arctic air. The models did not differ markedly in their forecasts of a strong baroclinic zone aloft initially oriented zonally across the central U.S. and developing a western ridge and eastern trough by the end of the 2-day forecast period. At the time of model initialization a strong surface ridge was already building southward into Texas from a 1052 mb center in the Yukon. By 12Z December 23 the ridge was also building eastward across the Ohio Valley and the Virginias (Fig. 12a). The 24-hour forecasts (Fig. 12b-d) show that the LFM significantly overbuilds the eastern branch of the ridge producing far too little development into Texas. In contrast the NGM at this time predicted building of the ridge that was too strong both to the east and south. Whereas the 1028 mb isobar verified as far east as extreme western Ohio and as far south as central Oklahoma, the NGM placed it in central West Virginia to the east and slightly to the south of Brownsville. The isentropic model produced the best forecast as seen by noting the very close proximity of the predicted and analyzed locations of the 1032, 1028, and 1024 mb isobars across the plains and the Ohio Valley.

By 12Z December 24 the massive ridge was pushing largely southward from a 1060 mb center in eastern Montana (Fig. 13a). The LFM is finally showing more southward development of the ridge yet the intensity and extent of the entire high pressure system are understated. Although the ridging over the Ohio Valley is still exaggerated in both the NGM and isentropic

model forecasts while the pressures in Texas are too low, they more accurately describe the overall intrusion of cold air than does the LFM. The NGM 48-hour forecast was superior in its prediction of the high's central pressure and of the strong pressure gradient along the ridge's western edge which reached from Texas to southern British Columbia.

e. Case 5: 12Z February 18, 1979

The nature and interaction of processes responsible for the explosive development of the President's Day cyclone and associated heavy snowfall have been discussed in considerable detail (Bosart, 1981; Bosart and Lin, 1984; Uccellini, et al., 1983, 1984). The storm arose through the establishing of a low level cyclogenetic environment from a combination of cold air damming east of the Appalachians concomitant with significant shoreward flow of oceanic moisture and heat followed by rapid spinup due to the approach of pronounced upper level positive vorticity advection and a mid and upper level potential vorticity maximum. Precipitation rates were enhanced by the presence of a low level jet coupled with the indirect circulation of a strong subtropical jet streak. The rapidity and complexity of this event make it a unique crucible for any numerical model.

The objective analysis of surface pressure by Bosart and Lin (1984) for 12Z February 19 and the corresponding 24-hour forecasts are shown in Fig. 14. By this time, what was a weak 1020 mb low only 12 hours earlier had moved northeast to a point just east of the Virginia coast and had spun up dramatically producing a central pressure of 1006 mb. The LFM prog showed a much weaker 1015 mb low located east southeast of Cape Hatteras. The NGM in a study by Guo and Hoke (1985) predicted the correct location of the low with a central pressure only four millibars greater than observed. The isentropic model also captured the rapid cyclogenesis by predicting the low's central pressure to within about one millibar of that analyzed but placed it slightly

too far offshore. As expected the latter two models also better described the amplitude of the thermal ridge than did the LFM.

The 12-hour cumulative precipitation fields verifying at 12Z February 19 (Fig. 15) show that the NGM produced the best forecast with the 0.5 inch isopleth agreeing fairly well with that of the observations. The LFM predicted no half inch totals but did place a 0.3 inch maximum in northern Virginia near the actual heaviest snowfall. Although the isentropic model produced a more accurate water equivalent maximum of 0.8 inches, it was located too far south and east. That both the low pressure center and precipitation maximum in the isentropic model's forecast were predicted too far seaward may partly be due to use of climatological rather than observed sea surface temperatures. The latter were not readily available but would likely have exhibited a stronger zonal gradient nearer to shore.

Given the marked contrast in surface conditions, the LFM's and isentropic model's winds aloft were surprisingly similar. Windspeed maxima at 700 mb and 300 mb were 5 to 10 m s^{-1} too slow while the cyclonic curvature over the North Carolina and Virginia coasts was too small, although more so in the LFM. The fact that forecast winds aloft were relatively similar suggests the importance of the models' treatment of processes within the lowest region of the atmosphere. While the isentropic model possesses two 50 mb sigma levels and generally four to seven predictive isentropic levels in the troposphere and the version of the NGM used in this case has eight such tropospheric levels (the current operational version has twelve), the LFM has a 50 mb boundary layer with only three additional tropospheric prediction levels. This difference in resolution in the lower region of the domains could have been a significant factor in the differing surface forecasts. Bosart (1981) previously suggested the potential importance of greater

vertical resolution in the troposphere for an event such as this, an idea supported by the numerical experiments of Nappi and Warner (1983) and Uccellini, et al. (1983).

4. Summary

A hybrid isentropic-sigma coordinate forecast model with a domain and numerical techniques very similar to those of the LFM II was used to generate forecasts of five diverse significant weather events for comparison with equivalent predictions by the LFM and NGM. The primary results of the experiments were as follows:

(1) In both cases involving springtime prefrontal convection, the most notable difference between model forecasts was in the low level moisture fields with the isentropic model consistently predicting the quantity, areal extent, and horizontal gradient of moisture more accurately than did the LFM or NGM. In that proper description of the water vapor field is essential to good precipitation forecasts, the fact that the LFM and NGM ultimately produced better rainfall predictions for these events was somewhat surprising.

(2) Both the NGM and isentropic model indicated small 12-hour rainfall maxima near a stationary convective cluster that was totally missed by the LFM. In the 24-hour forecasts, the NGM indicated rainfall considerably further north than observed while the isentropic model maintained a maximum relatively near the actual convection.

(3) Very strong surface ridging due to a major arctic cold surge was most accurately described by the isentropic model in the 24-hour forecast. By 48 hours all three models indicated the extent of the ridge with some degree of accuracy although the actual surface pressures were best predicted by the NGM.

(4) The LFM failed to predict the most critical aspect of the President's Day storm, i.e., the very rapid development of the surface cyclone off the East Coast. The position and intensity of the low were forecast well by the NGM as was the precipitation. While the central pressure was almost exactly correct in the isentropic model forecast, the low's position and associated precipitation were too far offshore.

Any conclusions drawn concerning the quality of a regional forecast model that are based on five cases are necessarily very preliminary. However, these events were the first five chosen for testing of the isentropic model, the only criteria for selection being diversity and a degree of challenge as forecast problems. The results suggest that improvements in pressure and moisture forecasts may be attained in at least some circumstances by describing mass, momentum, and water vapor transport in isentropic coordinates. More accurate moisture prediction would be particularly significant since development of models with this capability will be a necessary step toward improved severe weather and precipitation forecasts.

5. Acknowledgements

The author readily acknowledges the assistance of Dennis Deaven who provided both a detailed description of his original isentropic code as well as useful routines for post-processing results thus making feasible the development of the current isentropic model. Thanks are also extended to Ronald McPherson for his enthusiastic support of this work. Administrative support provided by Mary Chapman and Joyce Peters was much appreciated. This study was carried out under the auspices of the Resident Research Associateship Program of the National Research Council.

6. References

Black, T. L., 1984: Numerical experiments of jet streak ageostrophic circulations using pseudo-geostrophic initialization and perspectives. Ph.D. thesis, University of Wisconsin-Madison, 185 pp.

Bleck, R., 1974: Short-range prediction in isentropic coordinates with filtered and unfiltered numerical models. Mon. Wea. Rev., 102, 813-829.

_____, 1977: Numerical simulation of lee cyclogenesis in the Gulf of Genoa. Mon. Wea. Rev., 105, 428-445.

Bosart, L. F., 1981: The President's Day snowstorm of 18-19 February 1979: A subsynoptic-scale event. Mon. Wea. Rev., 109, 1542-1566.

_____, and S. C. Lin, 1984: A diagnostic analysis of the President's Day storm of February 1979. Mon. Wea. Rev., 112, 2148-2177.

Buzzi, A., A. Trevisan, and G. Salustri, 1981: Internal frontogenesis: A two-dimensional model in isentropic, semigeostrophic coordinates. Mon. Wea. Rev., 109, 1053-1061.

Charney, J. G., R. Fjortoft, and J. von Neumann, 1950: Numerical integration of the barotropic vorticity equation. Tellus, 2, 237-254.

Danielsen, E. F., 1959: The laminar structure of the atmosphere and its relation to the concept of a tropopause. Arch. Meteor. Geophys. Bioklim., All, 293-332.

Deaven, D. G., 1976: Solution for boundary problems in isentropic coordinate models. J. Atmos. Sci., 33, 1702-1713.

Eliassen, A., and E. Raustein, 1968: A numerical integration experiment with a model atmosphere based on isentropic coordinates. Meteor. Ann., 5, 45-63.

Gall, R. L., and D. R. Johnson, 1977: Prediction of a quasi-steady propagating jet core with an isentropic numerical model. Isentropic Numerical Models: Results on Model Development for Zonally Averaged and Secondary Circulations, Rept. to NSF, Dept. of Meteor., University of Wisconsin-Madison, 1-88.

Guo, X.-R., and J. E. Hoke, 1985: The impact of sensible and latent heating on the prediction of an intense extratropical cyclone--Some experiments with the nested grid model on the President's Day snowstorm of 18-19 February 1979. Office Note 314, National Meteorological Center, National Weather Service (NOAA), Camp Springs, Maryland, 19 pp.

Macpherson, A. K., M. H. Aksel, and P. D. Hilton, 1980: Study of frontogenesis using finite-element and finite-difference methods. Mon. Wea. Rev., 108, 1183-1196.

Nappi, A. J., and T. T. Warner, 1983: A numerical investigation of the President's Day storm on February 18-19, 1979. Preprints Sixth Conf. Numerical Weather Prediction, Amer. Meteor. Soc., Omaha, Nebraska, June 6-9, 1983, 298-305.

Petersen, R. A., 1979: Three-dimensional objective analysis using an isentropic cross-sectional technique. Preprints 11th Conf. Severe Local Storms, Kansas City, Amer. Meteor. Soc., 20-27.

Phillips, N. A., 1957: A coordinate system having some special advantages for numerical forecasting. J. Meteor., 14, 184-185.

Rossby, C.-G., et al., 1937: Isentropic analysis. Bull. Amer. Meteor. Soc., 18, 201-209.

Shapiro, M. A., 1975: Simulation of upper-level frontogenesis with a 20-level isentropic coordinate primitive equation model. Mon. Wea. Rev., 103, 591-604.

_____, and J. T. Hastings, 1973: Objective cross-section analyses by hermite polynomial interpolation on isentropic surfaces. J. Appl. Meteor., 12, 753-762.

Shuman, F. G., 1962: Numerical experiments with the primitive equations. Proc. Intern. Symp. Numerical Weather Prediction 7-13 November 1960, Meteor. Soc. Japan, 85-107.

Uccellini, L. W., and D. R. Johnson, 1979: The coupling of upper and lower tropospheric jet streaks and implications for the development of severe convective storms. Mon. Wea. Rev., 107, 682-703.

_____, P. J. Kocin, R. A. Petersen, C. H. Wash, and K. F. Brill, 1984: The President's Day cyclone of 18-19 February 1979: Synoptic overview and analysis of the subtropical jet streak influencing the pre-cyclogenetic period. Mon. Wea. Rev., 112, 31-55.

_____, R. A. Petersen, P. J. Kocin, M. L. Kaplan, J. W. Zack, and V. C. Wong, 1983: Mesoscale numerical simulations of the President's Day cyclone: Impact of sensible and latent heating on the pre-cyclogenetic environment. Preprints Sixth Conf. Numerical Weather Prediction, Amer. Meteor. Soc., Omaha, Nebraska, June 6-9, 1983, 45-52.

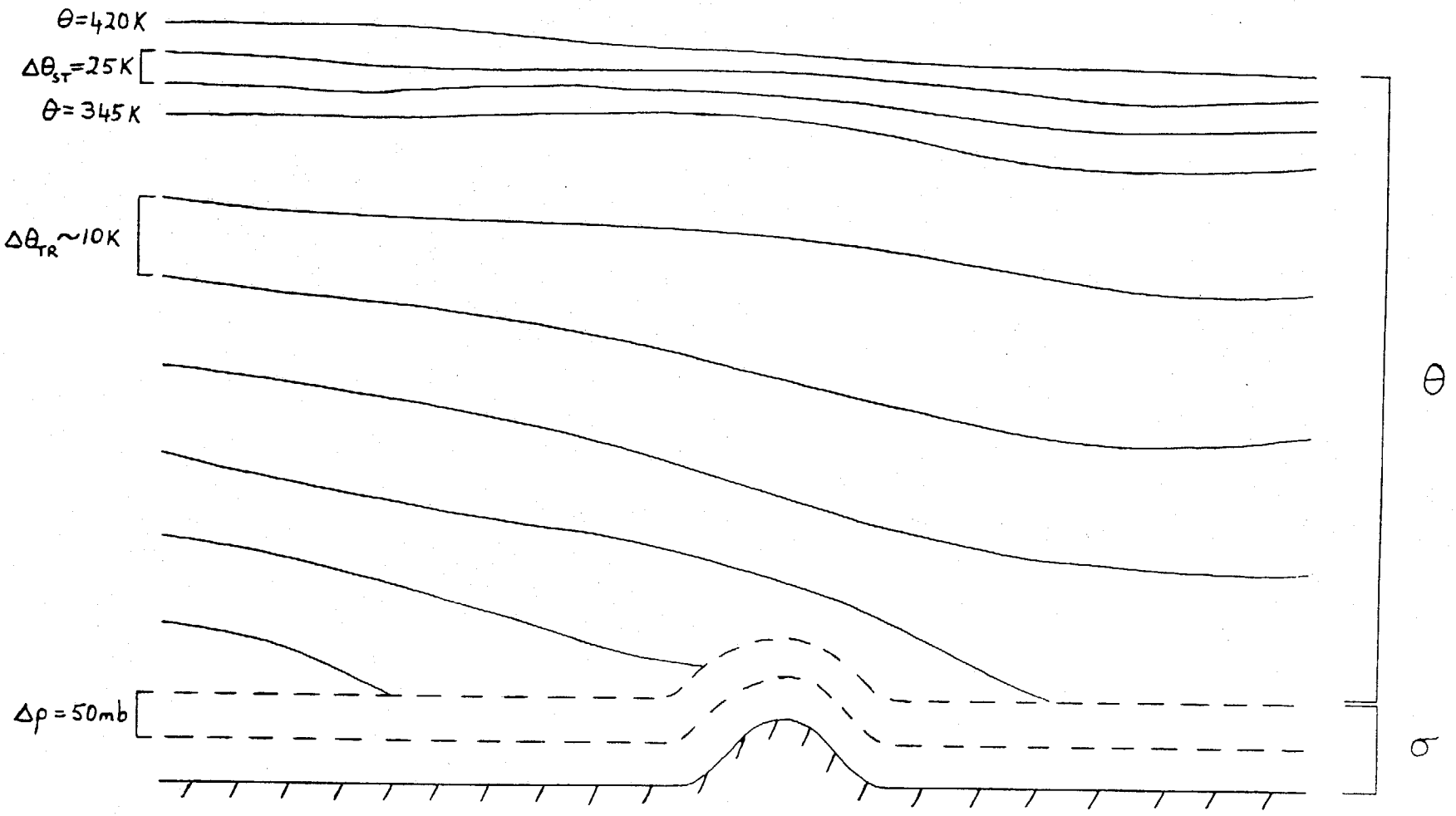

Fig. 1 Vertical cross section of isentropic model domain.

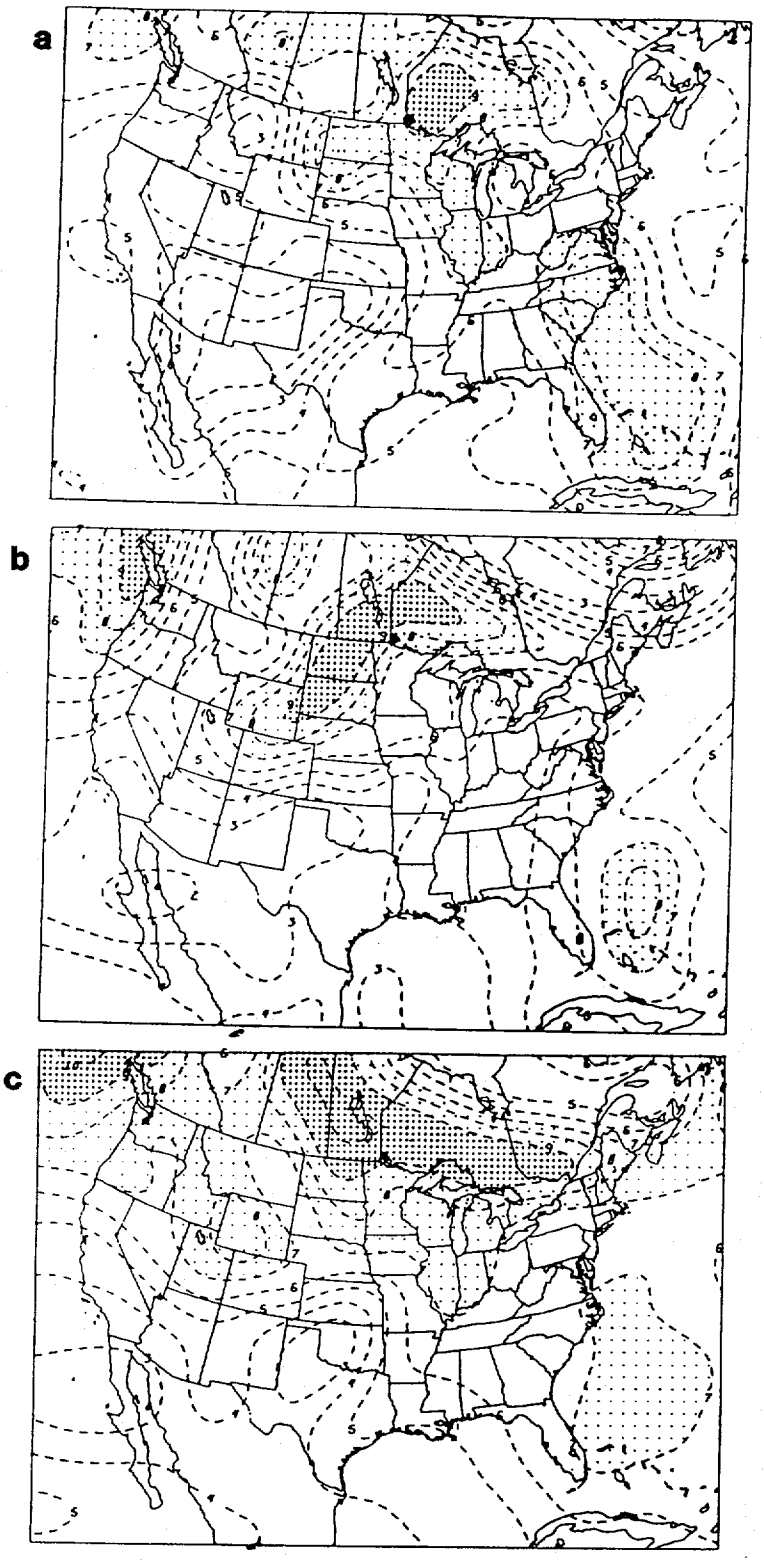

Fig. 2 Mean 1000-500 mb relative humidity at 00Z 12 May 1985: (a) LFM analysis; (b) LFM forecast; (c) isentropic forecast. Values are tenths of saturation.

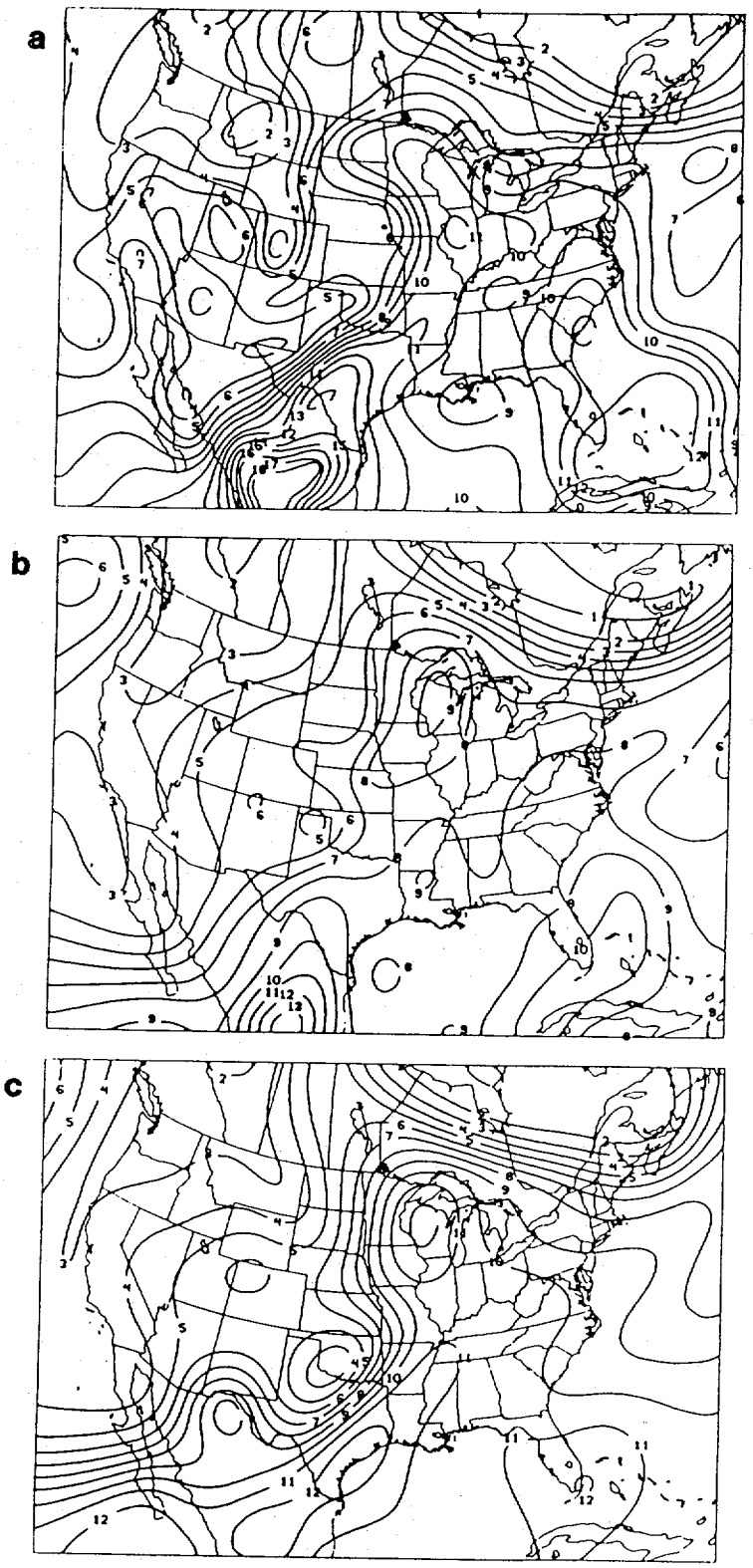

Fig. 3 The 850 mb specific humidity (g/kg) at 00Z 12 May 1985: (a) LFM analysis; (b) LFM forecast; (c) isentropic forecast.

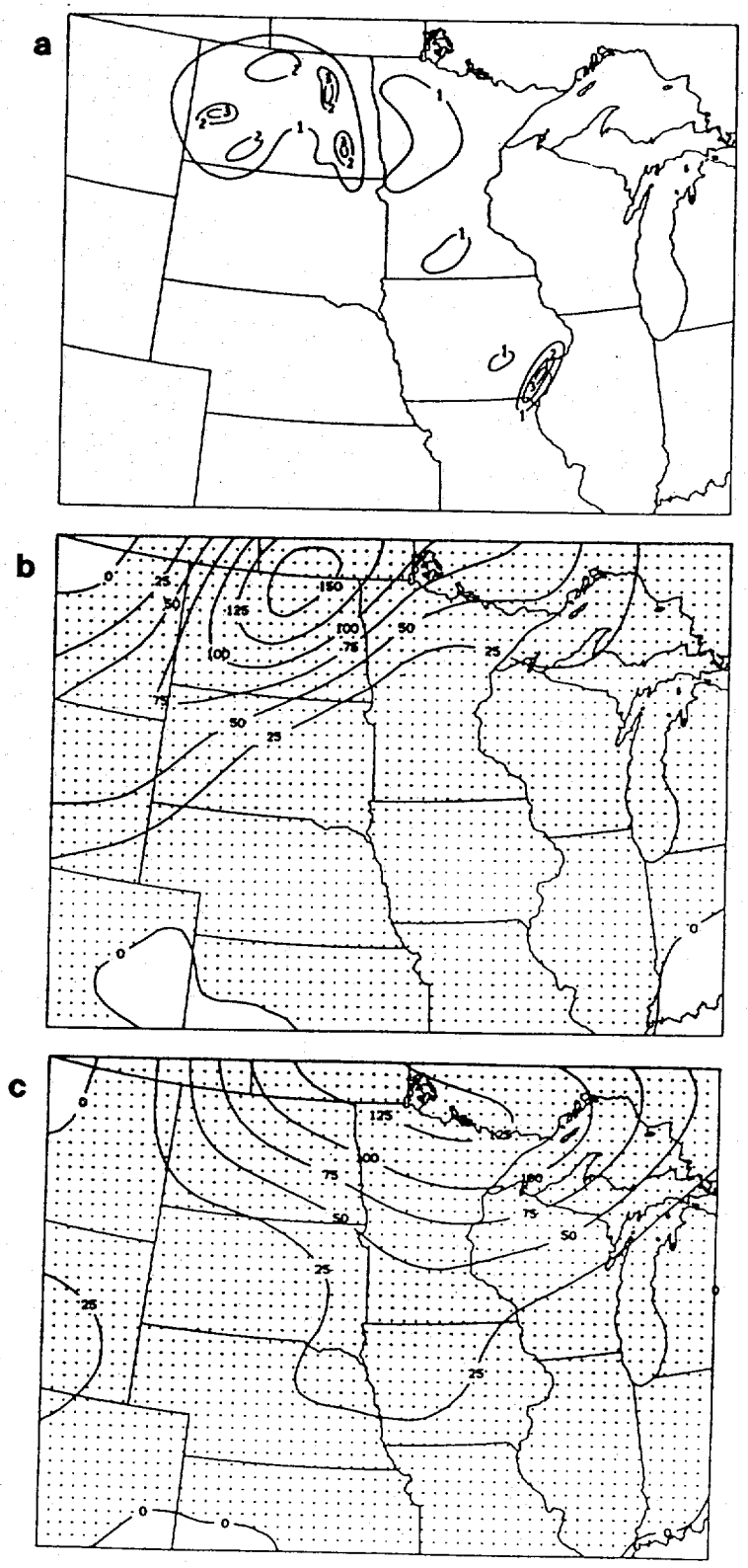

Fig. 4 Cumulative precipitation for 24-hour period ending 00Z 12 May 1985: (a) observed amounts exceeding one inch; (b) LFM forecast; (c) isentropic forecast. Units are inches in (a) and 0.01 inches in (b) and (c).

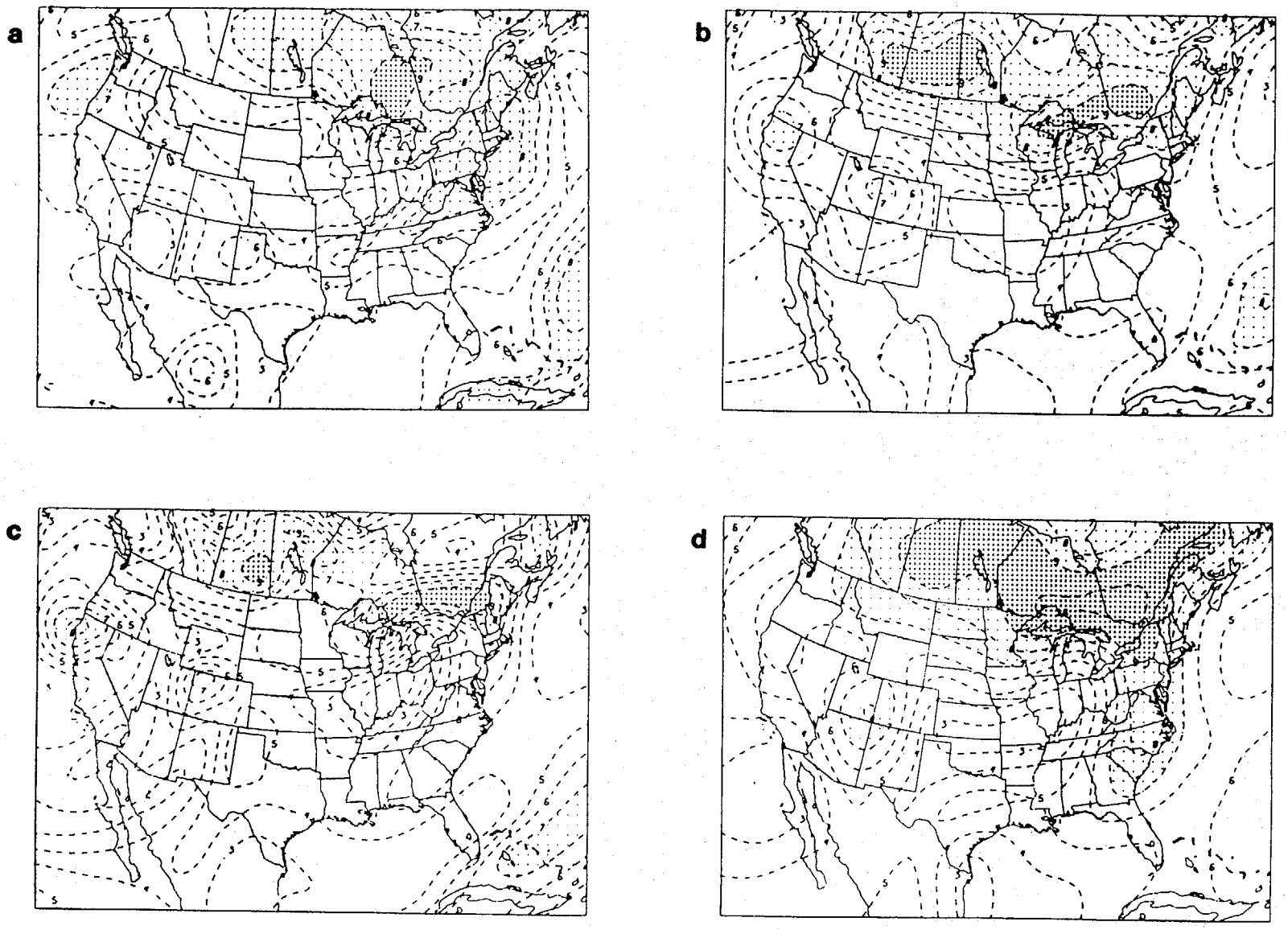

Fig. 5 Mean 1000-500 mb relative humidity at 00Z 1 June 1985: (a) LFM analysis; (b) LFM forecast; (c) NGM forecast; (d) isentropic forecast. Values are tenths of saturation.

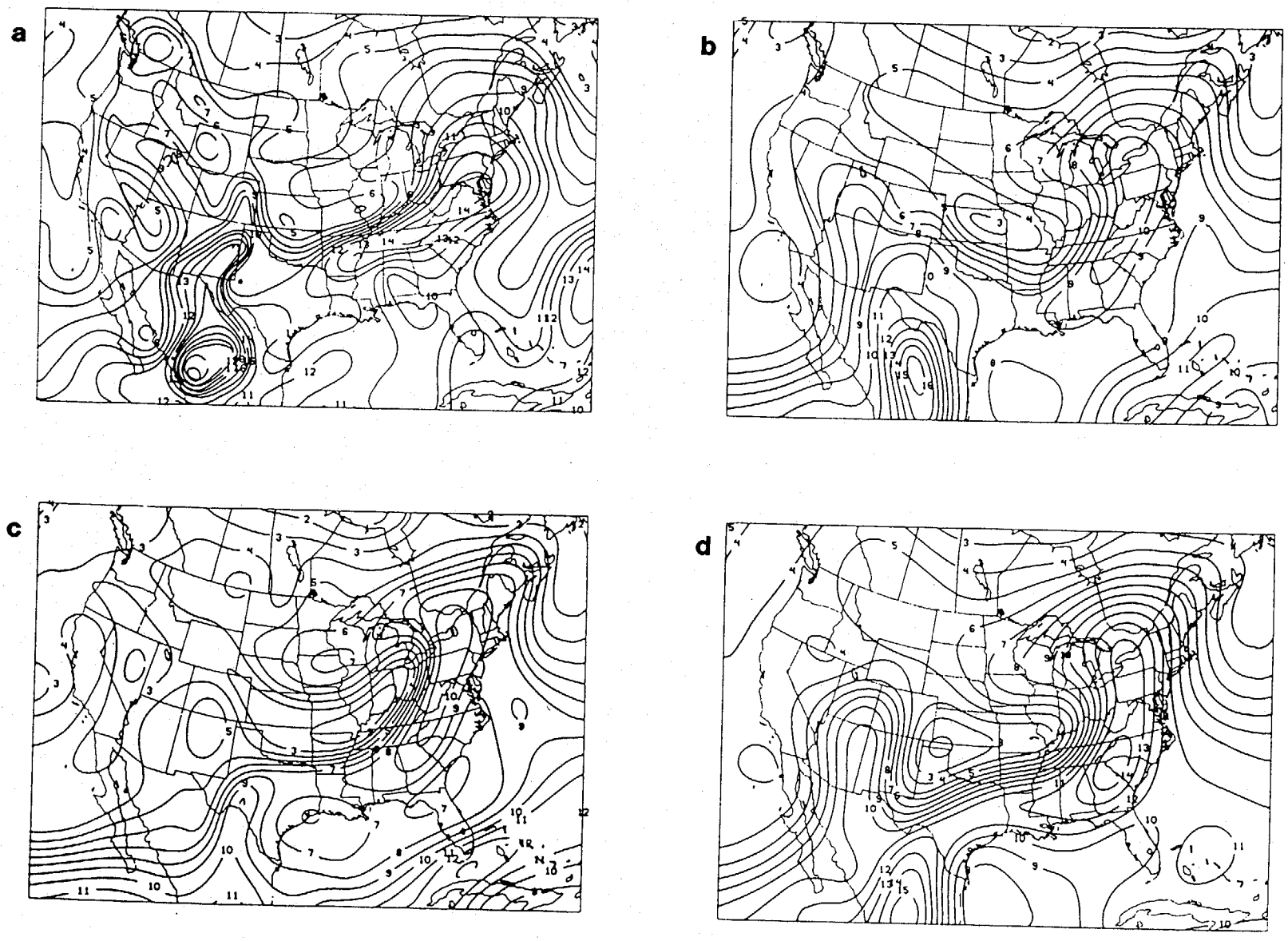

Fig. 6 The 850 mb specific humidity (g/kg) at 00Z 1 June 1985: (a) LFM analysis; (b) LFM forecast; (c) NGM forecast; (d) isentropic forecast.

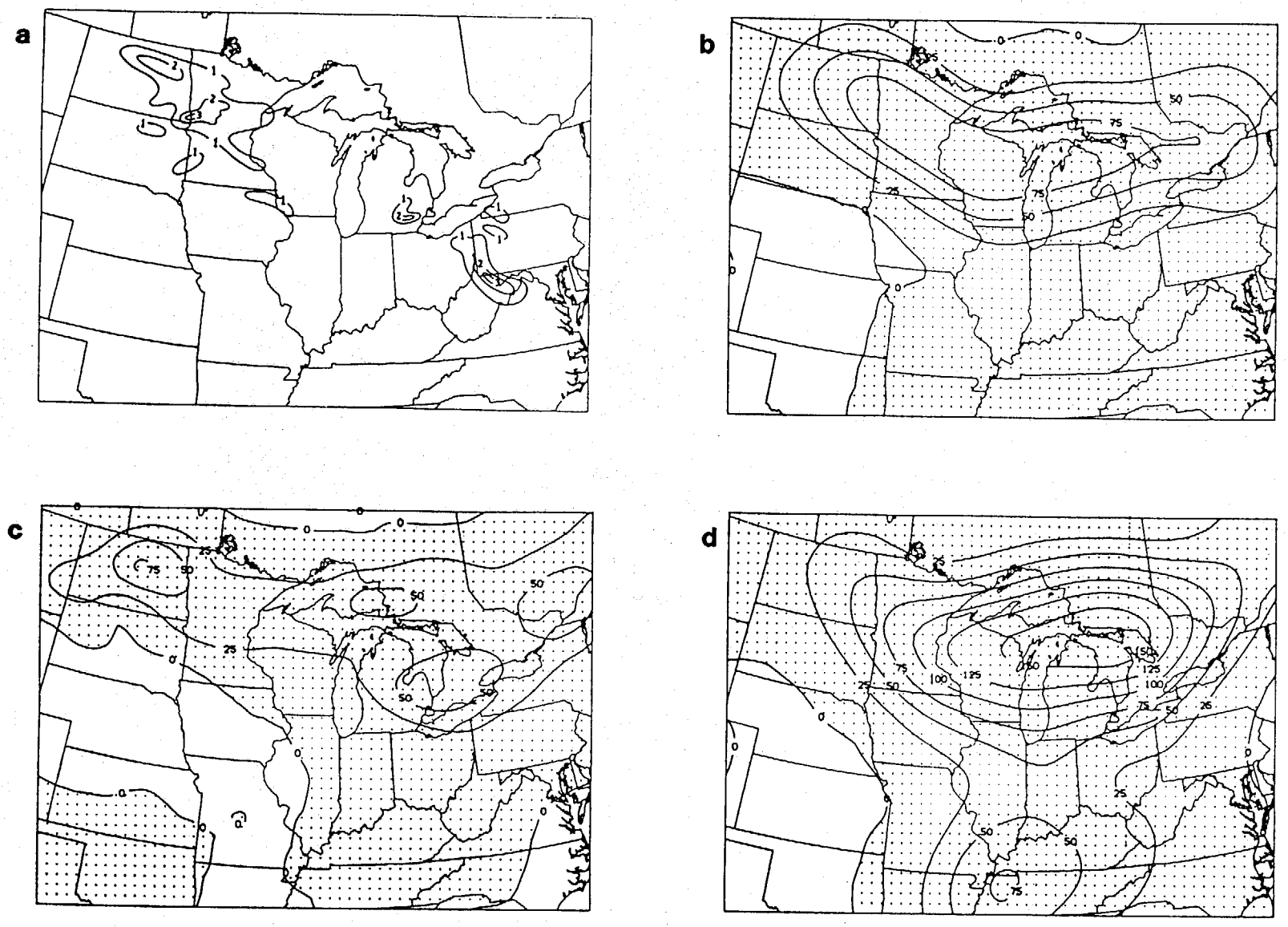

Fig. 7 Cumulative precipitation for 24-hour period ending 00Z 1 June 1985: (a) observed amounts exceeding one inch; (b) LFM forecast; (c) NGM forecast; (d) isentropic forecast. Units are inches in (a) and 0.01 inches in (b)-(d).

a

b

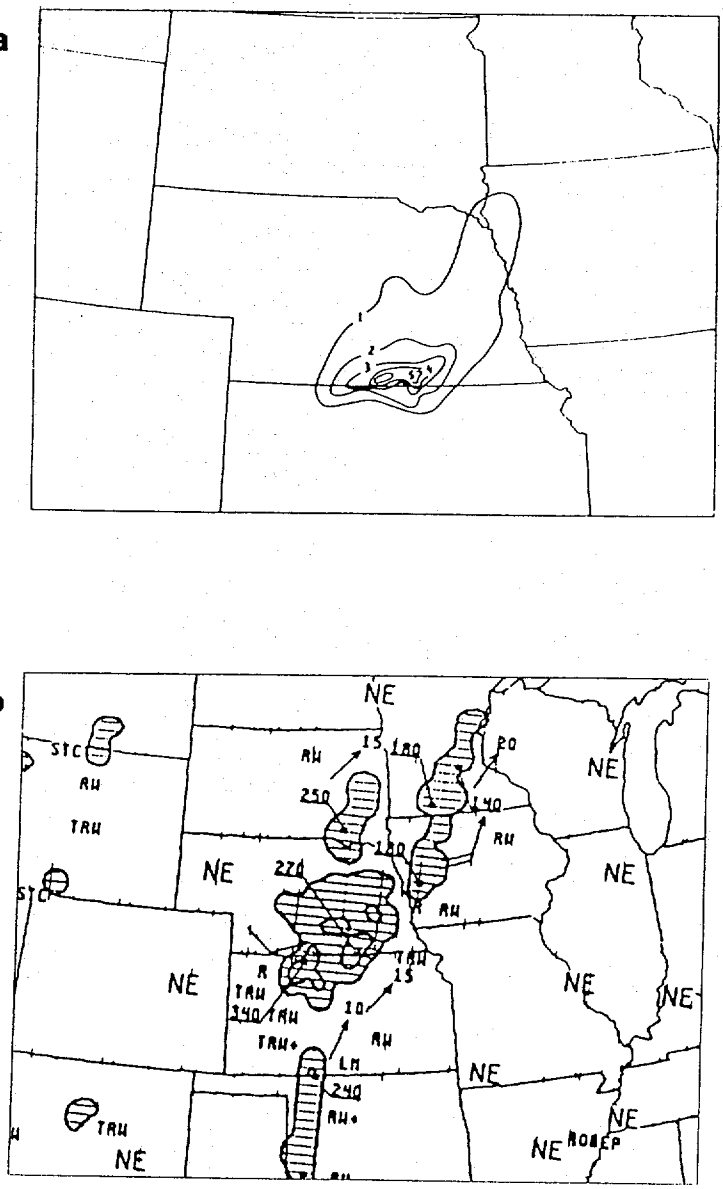

Fig. 8 (a) Observed cumulative precipitation (inches) for 24-hour period ending 12Z 29 September 1983. (b) Radar summary for 1135Z 29 September 1983.

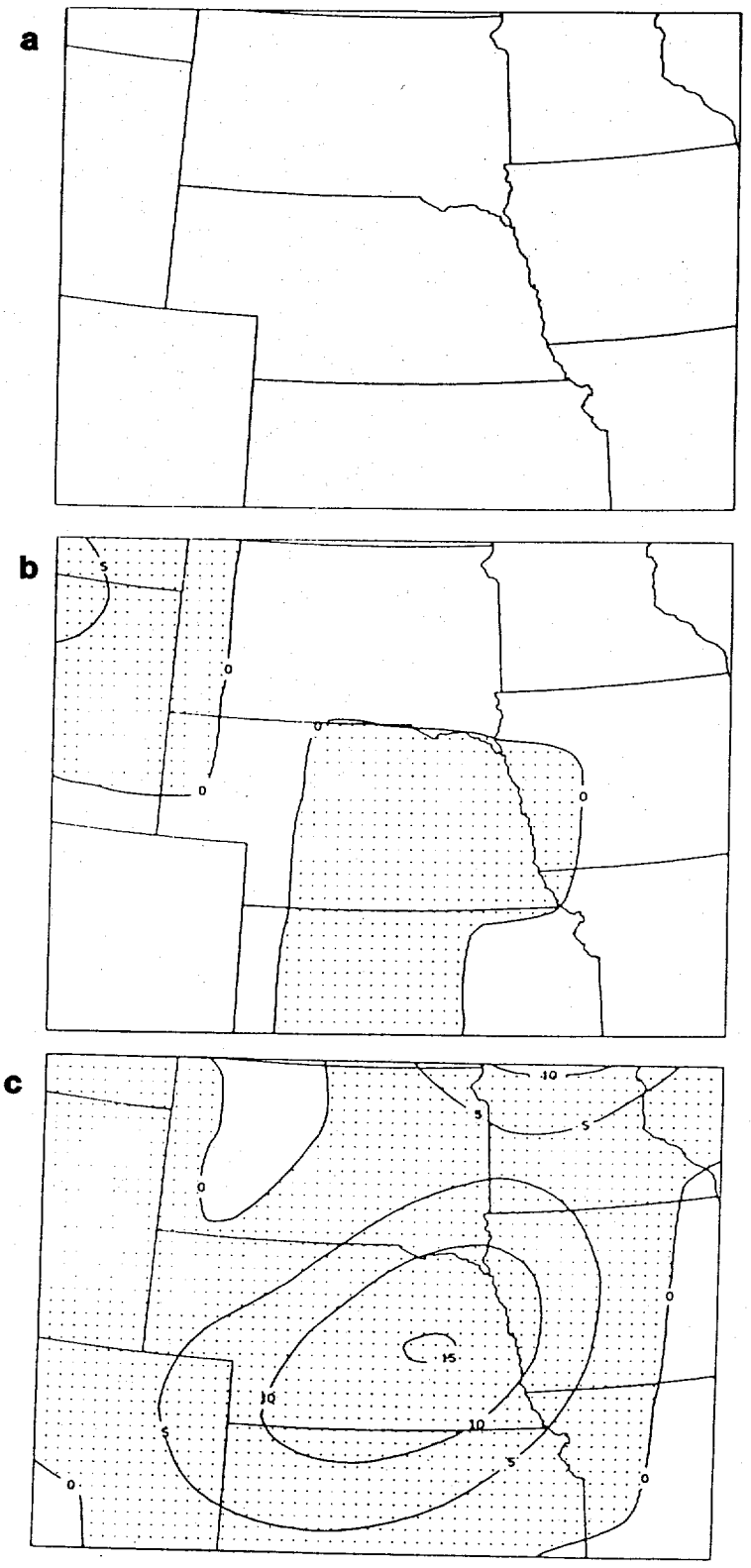

Fig. 9 Forecasts of cumulative precipitation (0.01 inches) for 12-hour period ending 00Z 29 September 1983: (a) LFM; (b) NGM; (c) isentropic model.

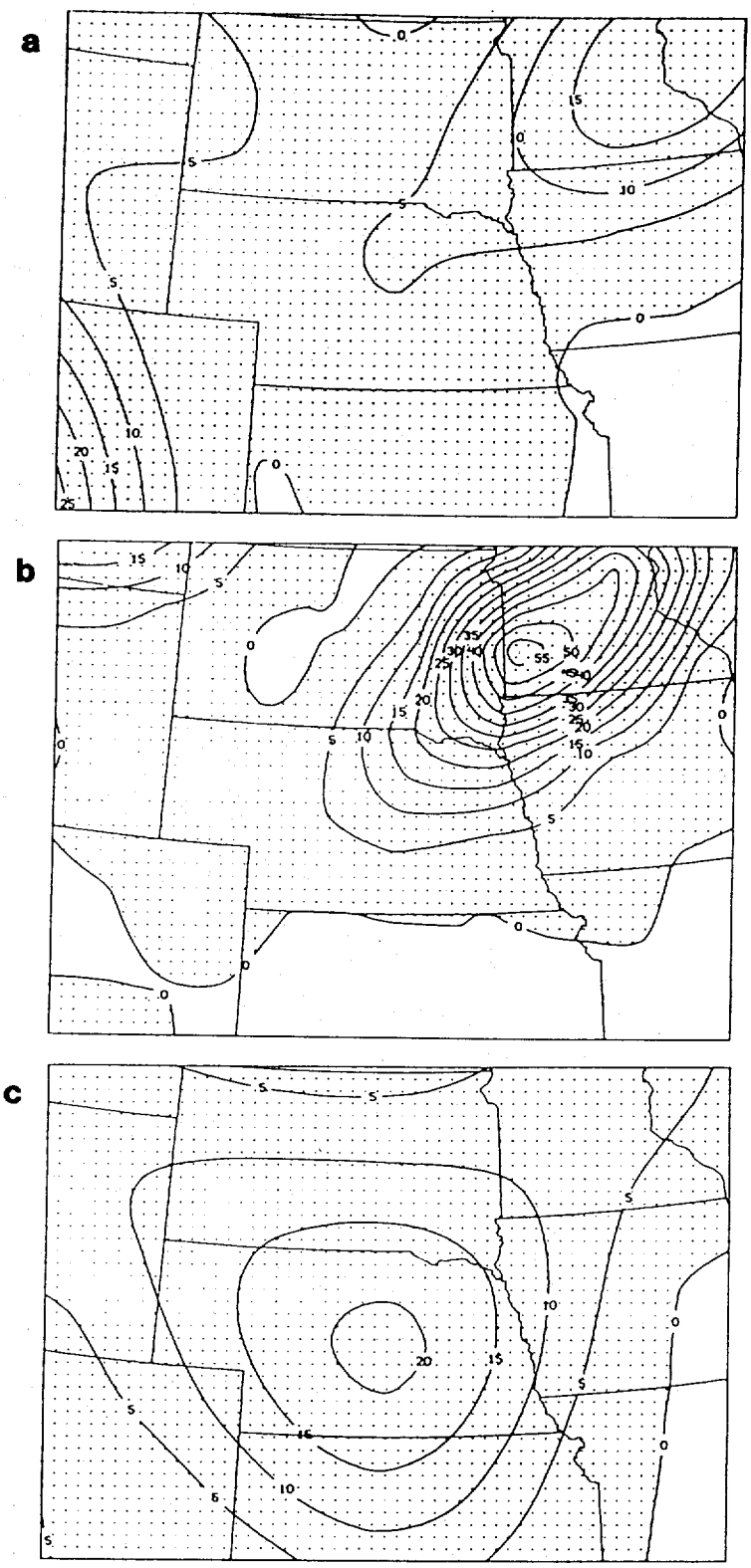

Fig. 10 Same as Fig. 9 except for 12-hour period ending 12Z 29 September 1983.

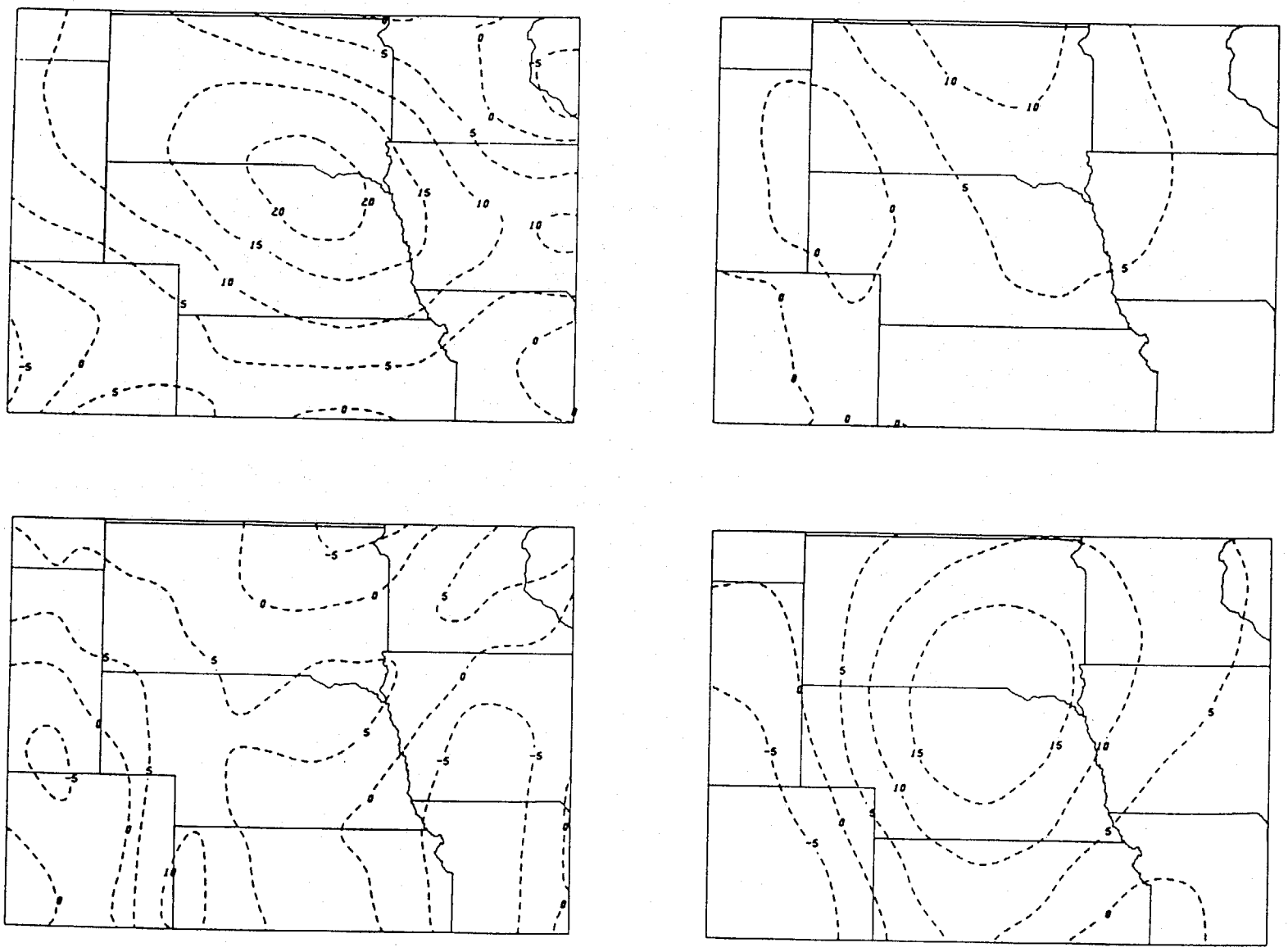

Fig. 11 The 300 mb velocity divergence (10^{-6} s^{-1}) at 00Z 29 September 1983: (a) LFM analysis; (b) LFM forecast; (c) NGM forecast; (d) isentropic forecast.

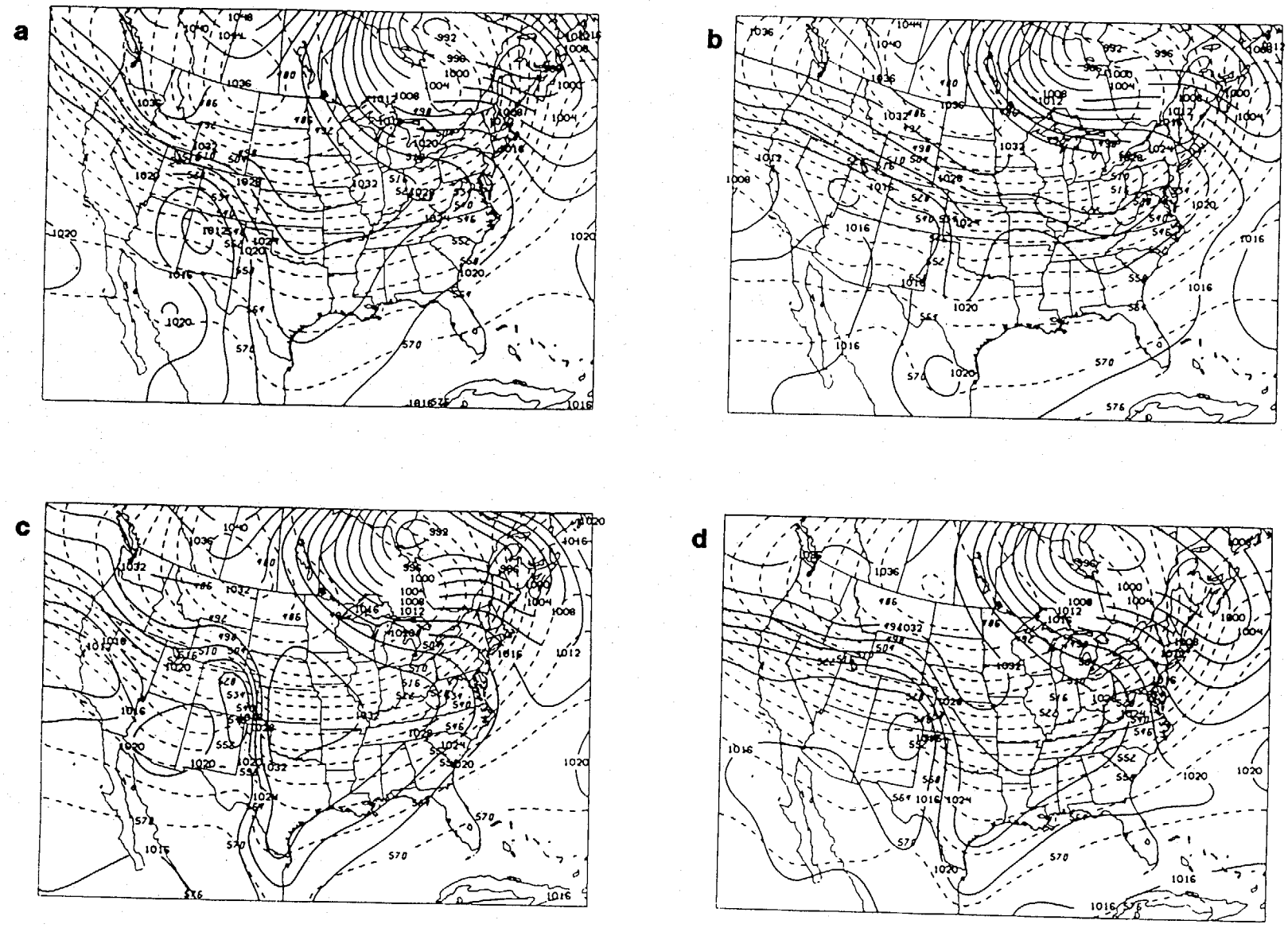

Fig. 12 Surface pressure (mb) and 1000-500 mb thickness (dam) at 12Z 23 December 1983: (a) LFM analysis; (b) LFM forecast; (c) NGM forecast; (d) isentropic forecast.

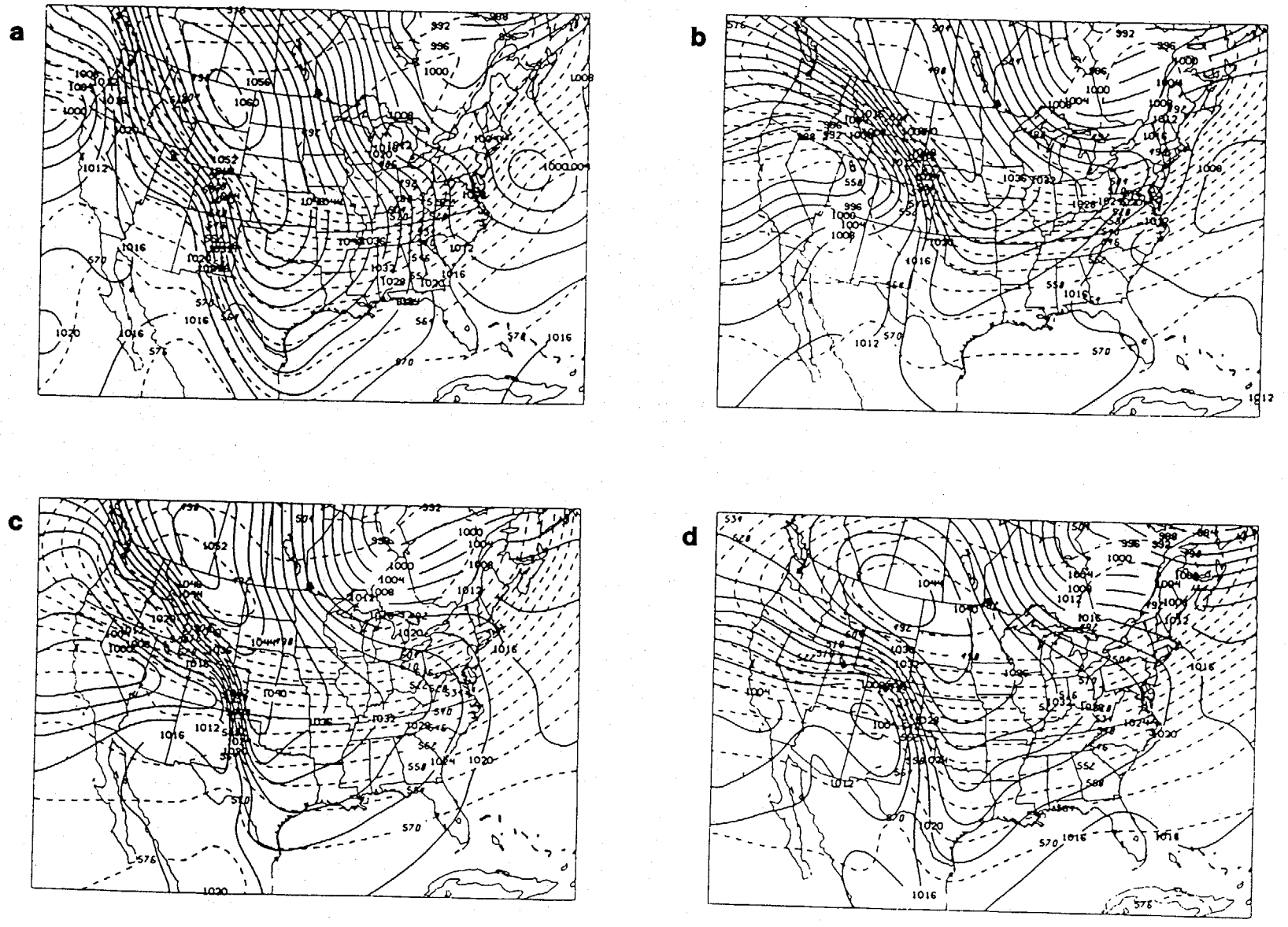

Fig. 13 Same as Fig. 12 except verifying at 12Z 24 December 1983.

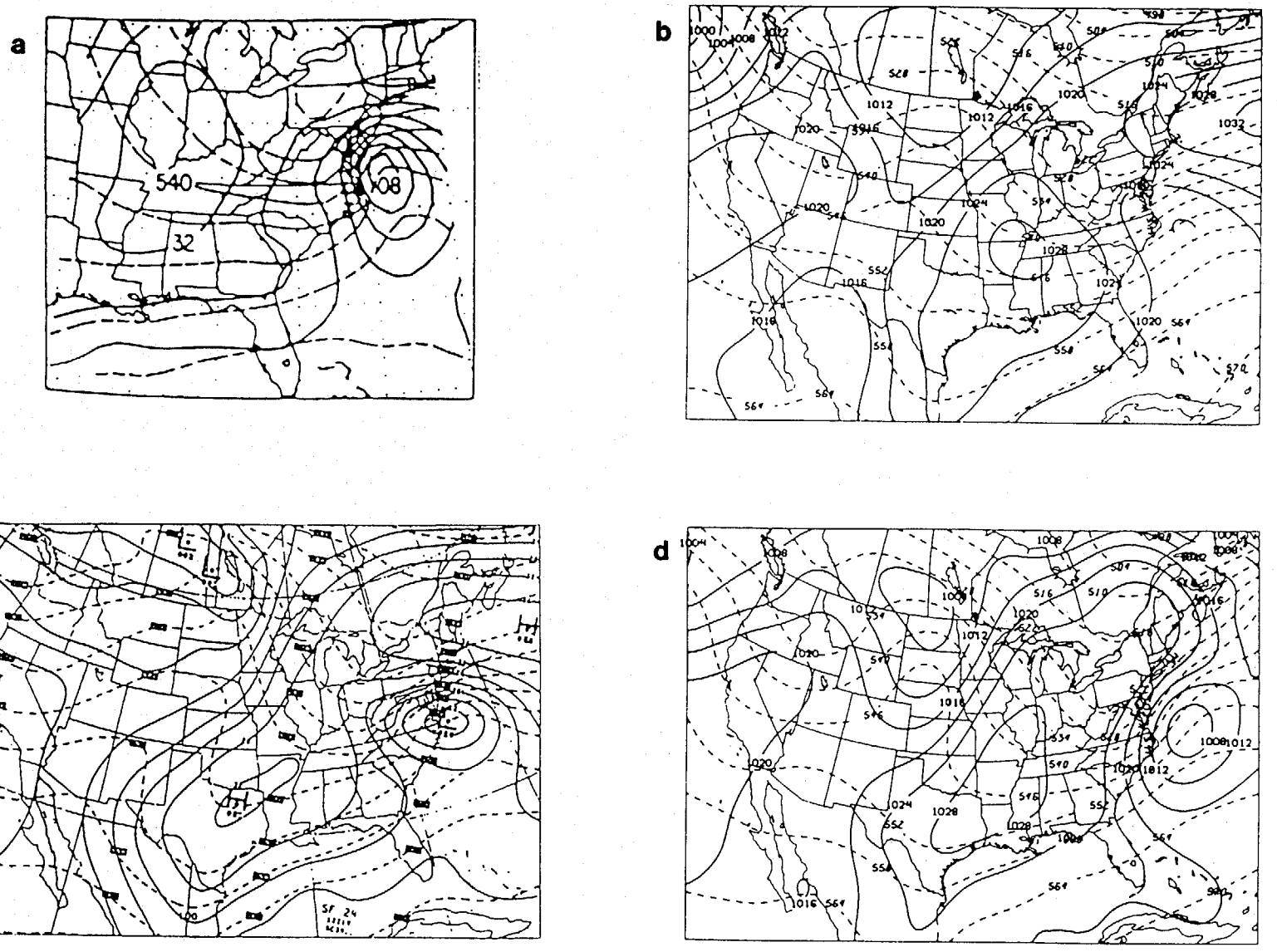

Fig. 14 Surface pressure (mb) and 1000-500 mb thickness (dam) at 12Z 19 February 1979: (a) objective analysis from Bosart and Lin (1984); (b) LFM forecast; (c) NGM forecast from Guo and Hoke (1985); (d) isentropic forecast.

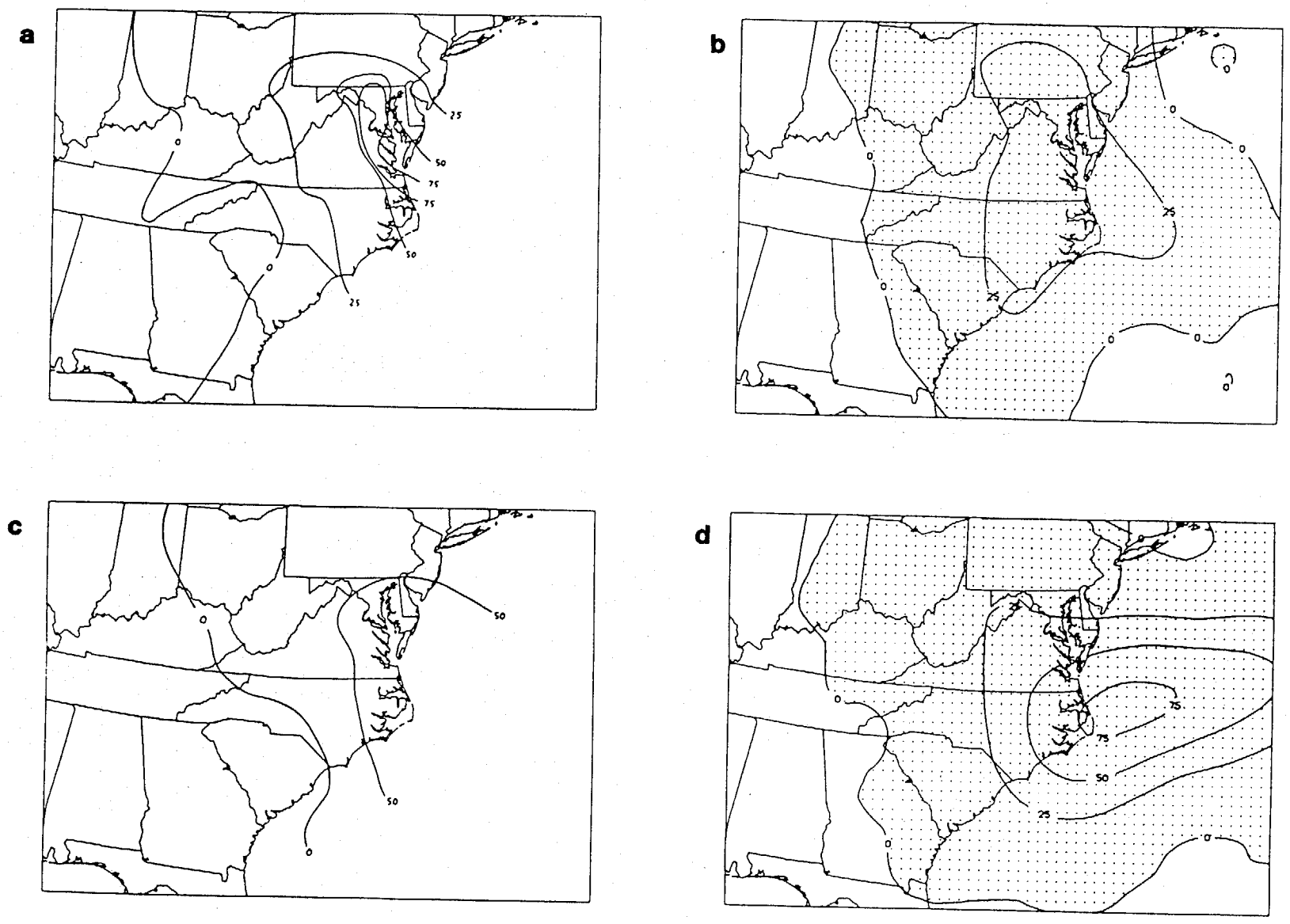

Fig. 15 Cumulative precipitation (0.01 inches) for 12-hour period ending 12Z 19 February 1979: (a) observed; (b) LFM forecast; (c) NGM forecast from Guo and Hoke (1985); (d) isentropic forecast.